

Modelling of tidal hydrodynamics for a tropical ecosystem with implications for pollutant dispersion (Cochin Estuary, Southwest India)

K.K.Balachandran^{*}, G.S.Reddy^{**}, C.Revichandran, K.Srinivas,

P.R.Vijayan and Tony J.Thottam

National Institute of Oceanography, Regional Centre, Cochin-682 018, India.

^{*} e-mail: kkbala@nio.org Tel: +91 484 2390814; fax + 91 484 2390618

^{**} Environ Software Pvt. Ltd., Wilson Garden, Bangalore 560 030, India.

Abstract

Tidal circulation in the Cochin Estuary, a moderately polluted estuary along the west coast of India, was studied using a 2D hydrodynamic model. The predicted tides and currents showed very good agreement with measured tides (RMS < 0.06 m) and currents (RMS < 0.07 ms⁻¹). The particle trajectories and residual currents computed from the model have been used to classify the study region into three zones: northern estuary, central estuary and southern estuary. The central estuary is dynamic, whereas the other two zones are relatively weak. An amplification of measured tides in the south estuary during March indicates the presence of standing waves caused by the hydraulic barrier at Thanneermukkom. The model results suggest that northern and southern zones showing flow restrictions are sensitive to environmental pollution. The present level of pollution in the northern estuary is due the direct release of industrial effluents into the river Periyar, which can be minimized if they are brought down to central estuary for disposal. The concept of different zones in the estuary will be useful to planners in protecting the vulnerable regions of this productive ecosystem from human interventions.

Keywords Cochin Estuary· Hydrodynamic model· Tides· Particle trajectory· Residual currents· Pollutant dispersion

1. Introduction

The Cochin Estuary (also called Vembanad Lake) is the second largest wetland ecosystem in India (Fig.1), sustaining rich bio-resources. The estuary gained its economic importance after the establishment of Cochin Port in 1936, but since then, has drawn environmental attention because of increased industrial pollution (Menon et al., 2000). The anthropogenic activities in the region started since the second part of 19th century onwards and remain high to the present day. During the early stages of developments in the country (1940s), industries were allowed to establish along the upper reaches of the estuary without understanding its complex hydrodynamics. Inadequate technology and high cost involved for waste water treatment eventually resulted in accumulation of pollutants, especially in the northern region (Qasim, 2003; Babu et al., 2006). Indiscriminate reclamation was another major intervention, which reduced the estuarine volume by 40% - an estimate made nearly three decades ago (Gopalan et al., 1983). The construction of salinity barriers in the upstream of the estuary to support agricultural activities during 1970's exacerbated the situation by reducing the flushing characteristics of the estuary and increasing the sedimentation. The annual maintenance dredging volume of $10 \times 10^6 \text{m}^3$ from the Cochin harbour region indicates the intensity of sedimentation (Rasheed, 1997; <http://www.cochinport.com/pdf/devinfo-projects.pdf>).

Recognizing its socio-economic importance, the Vembanad Lake has been included in the Ramsar site (No.1214) of vulnerable wetlands to be protected, in the year 2002 (<http://www.wetlands.org/R SIS/ COP9Directory/Directory/2IN019.html>). Restoration of this water body requires an understanding of the estuarine behavior, which can be achieved only through ecological modeling. Hydrodynamic modeling is a pre-requisite to the ecological modeling, as it influences the chemical and biological processes in the estuary significantly (Babu et al., 2005). The state of art of modeling in the Cochin Estuary is limited to an Estmorf model, which was less sensitivity due to the non-inclusions of bathymetry and river discharge (Strikwerda, 2004). The other two models (Eldho and Navin, 2004; Paul and Cvetkovic, 2007) are also limited to the Cochin harbour area and hence, do not contribute much to the tidal dynamics of the estuary. Keeping this in view, a modeling study has been carried out to understand the tide-driven currents of the Cochin Estuary during pre-monsoon (low river flow) and post-monsoon (high river flow) seasons using the model Hydrodyn-FLOSOFT.

Because of the complex topography, no effort has so far been made to study the dynamics of Cochin Estuary in total. Therefore, the present study by using a model will be the first of its kind. In this article, the results of hydrodynamic model, the classification of different estuarine zones with reference to tidal circulation including the significance of residual currents and particle trajectories are discussed.

2. Background

The Cochin Estuary constitutes a complex estuarine system (Fig.1), characterized by an ox-bow shape with its long axes running parallel to the coast and numerous islands (Soman, 1997). It is a bar-built micro tidal estuary receiving fresh water from 6 rivers ($20,000 \times 10^6 \text{ m}^3\text{y}^{-1}$, Srinivas et al., 2003a). The region receives about 320 cm rainfall annually, of which, nearly 60 % occurs during the southwest monsoon season (Qasim, 2003). The estuary is connected to the Arabian Sea at two locations, Cochin (Lat.9°58'N) and Azhikode (Lat.10°10'N) and is divisible into two parts: the southern arm extending from Cochin to the south and the northern arm extending from Cochin to Azhikode. The Cochin inlet is about 450 m wide, whereas Azhikode inlet is relatively narrow. During December to April, a salinity barrier at Thanneermukkom virtually cuts off the tidal propagation further south and modifies the circulation in the remaining part of the estuary. The important features of the southwest monsoon that vary from year to year are the onset date, quantity of rainfall and the duration of the season, which eventually result in the variability of estuarine characteristics, including water level and flow.

Information on the nature of tides and tidal currents in the Cochin Estuary are scanty and limited to the lower reaches (Wyatt and Qasim, 1973; Rama Raju et al., 1979; Varma et al., 1981, 2002). Fresh water influxes are found to influence the tides in the estuary (Joseph et al., 2007a). Harmonic analysis of tidal data showing an amplification of M₂ constituent in the southern estuary is attributed to the bottom frictional effects (Joseph et al., 2007b). The currents are generally dominated by semi-diurnal tides, which result in more swift currents than diurnal tides and play an important role in bed-load sediment transport (Srinivas et al., 2003 a). These currents are strongly rectilinear with a slack water at each reversal of direction. This slack water has important implications in the estuary, as settling of the finest fractions of sediments takes place at mid-tide (Srinivas et al., 2003b). Morphological history indicates that the estuary has a settling environment, as the sediments are shown to exhibit a

low to moderate energy regime in areas away from the river mouths (Priju and Narayana, 2007).

3. The numerical model

3.1. The governing equations

Since the estuary is shallow and vertically homogenous, a 2D model (Hydrodyn-FLOSOFT) is adequate to reproduce the tides and currents in the Cochin Estuary (Reddy, 1997; Vethamony et al., 2005; Babu et al., 2005). The following depth averaged equations of flow are solved numerically for the simulation of tides and currents.

Continuity equation is:

$$\frac{\partial n}{\partial t} + \frac{\partial uH}{\partial x} + \frac{\partial vH}{\partial y} = 0 . \quad (1)$$

where n = water elevation with respect to mean sea level, $H = (h + n)$ total water depth and h = water depth with respect to mean sea level.

The depth-averaged momentum equations in x and y directions are:

$$\frac{\partial uH}{\partial t} + \frac{\partial u^2H}{\partial x} + \frac{\partial uvH}{\partial y} = fvH - gH \frac{\partial n}{\partial x} + H \frac{\partial}{\partial x} \left(K_x \frac{\partial u}{\partial x} \right) + H \frac{\partial}{\partial y} \left(K_y \frac{\partial u}{\partial y} \right) + \frac{\tau_{wx}}{\rho} - \frac{\tau_{bx}}{\rho}, \quad (2)$$

$$\frac{\partial vH}{\partial t} + \frac{\partial vuH}{\partial x} + \frac{\partial v^2H}{\partial y} = -fuH - gH \frac{\partial n}{\partial y} + H \frac{\partial}{\partial x} \left(K_x \frac{\partial v}{\partial x} \right) + H \frac{\partial}{\partial y} \left(K_y \frac{\partial v}{\partial y} \right) + \frac{\tau_{wy}}{\rho} - \frac{\tau_{by}}{\rho}, \quad (3)$$

where t = time; x, y are Cartesian co-ordinates; u and v are depth averaged velocity components in the x and y directions, respectively; f = Coriolis parameter; g = acceleration due to gravity; K_x, K_y diffusion coefficients in the x and y directions, respectively; τ_{wx}, τ_{wy} and τ_{bx}, τ_{by} = wind and bottom stresses, respectively in x and y directions; ρ = density of sea water.

3.2. Boundary-Fitted-Coordinate (BFC) system

In the Cartesian or rectilinear co-ordinate system, it is difficult to represent the complex coastline accurately, as grid size remains the same at any given location. In the present study, BFC system has been used to resolve complex topography in horizontal

direction (Fig.2). The continuity equation can be written in BFC system using chain rule transformation as:

$$\frac{\partial n}{\partial t} + \frac{1}{J} \left(y_{\eta} \frac{\partial(uH)}{\partial \zeta} - y_{\zeta} \frac{\partial(uH)}{\partial \eta} + x_{\zeta} \frac{\partial(vH)}{\partial \eta} - x_{\eta} \frac{\partial(vH)}{\partial \zeta} \right) = 0, \quad (4)$$

where, $x_{\eta}, y_{\eta}, x_{\zeta}, y_{\zeta}$ = grid transformation parameter, and J = Jacobian transformation. The momentum equations can also be written in BFC coordinate system in the same manner as described above (Thomson et al., 1977; Reddy, 1997, Vethamony et al., 2005).

The transformed governing equations of flow have been discretised on a staggered grid and solved using Alternating Direction Implicit (ADI) finite difference scheme. The scheme splits the time into two intervals. In the first half-time step, derivatives with respect to ζ are advanced from t^n to $t^{n+1/2}$, and the derivatives involving η are held at t^n . In the second half-time ζ derivatives are held at $t^{n+1/2}$ and η derivatives are advanced from $t^{n+1/2}$ to t^{n+1} . Non-derivative terms are computed at t^n for both levels. The transformed equations of flow are discretised using ADI procedure in ζ and η directions, arranged in the form of algebraic equations and grouped together to form a tri-diagonal matrix, which is then solved implicitly for tides and currents. The time step (Δt) is chosen based on the Courant stability criteria because, the BFC grid size varies both in x and y directions. In this study, the time step is considered to vary from 10 to 15 seconds, according to changes in the velocity and grid.

3.3. Model set up

The various steps required to setup the model are grid generation, initial and boundary conditions and horizontal diffusion coefficients. The computational domain of the model is selected from north of Cochin Estuary to Thanneermukkom bund between Lat: 9°39'07''N, Long: 76°20'E and Lat: 10°07'33''N, Long. 76°11'06''E. The grid is a curvilinear mesh and non-uniform both in x and y directions (Fig. 2). The grid size varies from 30 to 50 m and accordingly, the area of computational cells varies from 900 to 2500 m².

Bathymetry of the southern estuary (between 10 km south of the inlet and Thanneermukkom) was measured during a field survey in April 2003 using an echo sounder (Ceeducer, accuracy ± 0.03 m) interfaced to a differential GPS (accuracy ± 0.30 m). Tidal

corrections were made to the observed depths and reduced to chart datum. The bathymetric data of the harbour region was obtained from the map of Cochin Port Trust and that of the northern estuary was extracted from the hydrographic charts of Inland Waterways Authority of India, Cochin. Compilation of all bathymetric data into a single domain with interpolated bathymetry (Fig.1) was achieved through the Hydrodyn-FLOSOFT software.

The initial state for the model is based on still-water conditions. The boundary conditions selected are (i) observed tide at the Cochin inlet (9°59' N; 76°16' E) during October 2003 (post-monsoon) and March 2004 (pre-monsoon) and, (ii) no flux across the southern and northern boundaries. Diffusion coefficients for horizontal exchange of momentum are considered to vary spatially. The hydrodynamic model was forced using the time series hourly tide data observed at the Cochin Port Trust (Stilling well tide gauge) for the period 6 to 31 March 2004 (Fig.3). As the observed tides are available at larger time interval, cubic spline interpolation technique has been applied to calculate the value at each computational time step.

The horizontal diffusion coefficients K_x and K_y are calculated as:

$$K_x = \alpha_x g (\sqrt{u^2 + v^2}) / C^2 \quad (5)$$

$$K_y = \alpha_y g (\sqrt{u^2 + v^2}) / C^2 \quad (6)$$

where, $\alpha_x = 0.15$ and $\alpha_y = 0.15$ are the depth averaged eddy viscosity coefficients in x and y directions and C (in m^{1/2}/s) is the Chezy coefficient. The diffusion coefficients for horizontal exchange of momentum vary in space. The wind stress in the x and y directions (τ_{sx}, τ_{sy}) can be written as:

$$\tau_{wx} = \rho_a C_d U_w \left(\sqrt{U_w^2 + V_w^2} \right) \quad (7)$$

$$\tau_{wy} = \rho_a C_d U_w \left(\sqrt{U_w^2 + V_w^2} \right) \quad (8)$$

where, $U_w, V_w =$ wind velocity components in x and y directions respectively, $\rho_a =$ air density, $C_d =$ air water drag coefficient. The bottom stress in the x and y directions (τ_{bx}, τ_{by}) can be written as:

$$\tau_{bx} = gu \left(\sqrt{u^2 + v^2} \right) / C^2 \quad (9)$$

$$\tau_{by} = gv \left(\sqrt{u^2 + v^2} \right) / C^2 \quad (10)$$

where, τ_{bx} , τ_{by} = bottom stress components in the x and y directions respectively and, u , v = depth averaged velocity components in the x and y directions respectively.

4. Results

4.1. Model calibration and cross validation

The computational runs have been carried out using various bed roughness coefficients (combined effect of median sediment particle size or d_{50} and bed configuration) in order to calibrate the model with respect to the tide data of March 2004. In the present study, a constant Manning's roughness coefficient (0.003) was found to be suitable. The simulated tides are compared with measured tides at Bolghatty, situated 6 km interior from the inlet in the northern estuary. The comparison gave good correlation in phase and amplitude (root mean square deviation, RMS = 0.058 m; variance explained, VE = 94%; n = 600). Similarly, the simulated currents are compared with currents measured using RCM9 current meter deployed 2 m below the surface at Bolghatty (Fig.3). The magnitude as well as directions of both measured and simulated currents show a very good match (RMS = 0.068 ms^{-1} ; VE = 89%; n = 600). Comparison has also been made with simultaneous water level data collected at 6 critical locations (Fig.4) inside the estuary (Thevara, Vaduthala, Makyil Kadavu, Vaikom, TV Puram and Thaneermukkom) during the day time (0600 – 1800 h; Data source: The State Irrigation Department, Thiruvananthapuram and Inland Waterways Authority of India, Cochin).

The model after calibration has been subjected to a cross validation by predicting the water levels at the same locations during a high river flow period (October 2003). During these simulations, none of the parameters of the model were changed. Hence, the increase in the monsoon river flow through the southern boundary and the consequent changes in the bed roughness are not considered. It can be noted from Table 1 that during October also, the model results (Fig.5) are comparable with water levels ($0.05 \leq \text{RMS} \leq 0.11$) showing that the

model is capable of reproducing the tides in the Cochin Estuary reasonably well. The results can be improved further by including the river flow, winds and bottom drag for the corresponding period.

Apart from predicting the propagation of tides, the model identifies some of the fine features appearing in the estuary. In a mixed semi-diurnal tide with very large diurnal inequality, the higher low water level (or lower high water level) frequently becomes indistinct. During these periods, the diurnal tide has such an overriding dominance that the semi-diurnal, although still present, cannot be seen on the tidal curve (Srinivas et al., 2003a). This tide, often referred to as the *vanishing tide*, could be seen on 17th March, 30th March (Fig. 3, 4) and 4th October and 20th October (Fig. 5), indicating the sensitivity of the model.

From Fig.3, it can be noticed that while the predicted tides show very good agreement, the observed flood velocities are slightly higher than the predicted flood velocities. The predicted velocity generally shows that there is no appreciable change in the tidal propagation speeds in the estuary during October and March (Fig.4, 5), but there are some regions where the average currents are always swift (Cochin inlet to Vaduthala) or always slow (south estuary and north estuary). The variation in the speed could be due to the changes in topography and cross sectional area, particularly to the south of Vaduthala (Strikwerda, 2004). The distribution of water levels during various phases of tides indicates a recurrence of resident water mass alternately in the south estuary and north estuary. To illustrate this peculiar behavior, the predicted water levels and average currents during ebb tides of two neap phases during October and March are furnished in Fig.6 and Fig. 7.

The ebb tide during October (Fig.6) show that relative to the Cochin inlet, the water levels of the north estuary, southern estuary and Vayalar estuary are elevated by 0.01, 0.10 and 0.13 m, respectively. Consequently, the ebb currents between Vaduthala and Cochin (0.11 to 0.15 ms^{-1}) are swift, which render momentum to the central estuary, extending further north up to Bolghatty (marked as “ \leftrightarrow ” in Fig.6). These currents are however, weak in the northern and southern estuary. It implies that the water level rise in the south estuary do not correspondingly increase the ebb currents. In an identical situation during March also, the water levels (Fig.7) in the south estuary and Vayalar estuary are relatively elevated by 0.23 and 0.31 m respectively, whereas they are low in the inlet and north estuary (0 and 0.03 m, respectively). Here again, swift currents (marked as “ \leftrightarrow ” in Fig. 7) prevailed in regions between Vaduthala and Cochin ($0.12 - 0.40 \text{ m.s}^{-1}$), whereas it continued to be weak in the

northern and southern estuary. The situation changes during flood tide, when the water levels between the Cochin inlet and north estuary are relatively higher than the rest of the estuary (figure not shown).

The common features observed during the two instances are the pressure head in the south estuary and strong ebb currents between Cochin and Vaduthala, in contrast to weak currents on either sides (south estuary and north estuary). The weak flow in the south estuary in spite of the water elevation could be attributed to the topography, where the estuary branches out into a wide area including that of Vayalar estuary.

4.2. Residual currents and tidal excursions

The net tidal transport is characterized by the residual currents exchanged between regions within the estuary resulting from the net transport, averaged over one or many tidal cycles (Murray et al., 2003). These currents are typically one or two orders of magnitude less than the instantaneous currents, and are generated through the interaction of the tidal currents with topography (Pugh, 1987; Emery and Thompson, 1997). Fig.8 shows the residual currents for October 2003 based on a 14.5 day simulation (2 to 16 October) of the model. It is evident that the region between Vaduthala and Cochin (up to Bolghatty) shows a net export from the estuary, whereas further towards the south estuary and north estuary, the residual currents are weak.

Tidal excursion (particle trajectories) provides an approximate distance traveled by an immiscible particle for a period of 14.5 days (Taguchi and Nakata, 1998). The tidal excursion at the surface is simulated using the model as trajectories of Lagrangian particle tracers released at various locations in the estuary during October 2003 and March 2004. Figure 9 shows that on both occasions after 14.5 days, the particles released at locations 3 to 6 (Cochin inlet to Vaikom) have undergone large horizontal shifts (> 2000 m), whereas the shifts are smaller in other locations. This means that the tidal excursion is faster between Cochin and Vaikom, but slower in the north and south estuaries. Hence, these locations (1, 2, 7, 8, 9,10) could be weak in their dispersion characteristics, which in turn, have implications on the pollutants discharged into the estuary at these locations.

The major factors influencing the propagation of tides in an estuary are the topography, depth and river flow. Generally, the tides entering through the inlet would be progressively attenuated as they propagate upstream. In contrast, the observed water levels in

the Cochin Estuary, especially during March, are found to increase conspicuously beyond 32 km (Vaikom to Thanneermukkom, Table 1, Fig. 4). Based on a relative scale, the water levels at the Cochin inlet (1.01 m) is reduced to 0.53 m at 27 km south (Makyil Kadavu), from where it gradually increased to 0.70 - 0.72 m between Vaikom and TV Puram (by 0.17 m). This kind of tidal amplification observed in the south estuary during March is possibly caused by the closure of the hydraulic barrier at Thanneermukkom. The tidal elevation during October 2003 (Fig.5) is however, less prominent (0.12 m), possibly due to the non-tidal influence (river flow).

5. Discussion

A comparison of the results from the tides, tidal currents and tidal excursions reveal that the present model explains the tidal characteristics of the Cochin Estuary satisfactorily. The better agreement in predictions of tides during March 2004 as compared to October 2003, is due to the insignificant river discharge during the former period. On both occasions, the model predicts swift currents between Cochin inlet and Vaduthala, while weak currents are predicted on either parts of the estuary (Fig.6 and 7). The Lagrangian particle trajectories also indicate that particles released between Cochin inlet and Vaduthala undergo relatively large horizontal displacement (Fig. 9 and 10). Thus, all the simulations uniformly suggest that the region between Cochin inlet and Vaduthala is dynamic. The weak flow in the south and north estuaries, located outside this central region, is probably caused by the unique topography, which leads to distinct circulation patterns in the northern and southern parts of the estuary (Ramamirtham et al., 1986 a & b).

The Cochin Estuary is wide and deep in the south but, shallow and net-worked towards north. It is therefore assumed that, the tides entering through the Cochin inlet undergo modifications in the south estuary, due to the wide storage area to the south of Vaduthala (Strikwerda, 2004). The closure of the hydraulic barrier at Thanneermukkom during pre monsoon season (March) leads to the formation of standing waves in the south estuary. This is a marked deviation from the hydrodynamics of Mandovi-Zuari estuary, another tropical estuary located approximately 800 km north of Cochin Estuary, where the tidal heights remain unchanged for large distances (40 km from the mouth), as a result of balance between geometric amplification and bottom friction (Shetye et al., 1995; Unnikrishnan et al., 1997). Features like irregular bathymetry, tidal flats and bottom friction are found to amplify the tides in Keum River estuary (Ye and Johnson, 1994; Kang and Jun,

2003) and Pearl River estuary (Qingwen et al., 2004). Construction activities including reclamation within a choked estuarine embayment could also lead to tidal amplification and flow restriction (Byun et al., 2004).

Based on the differential responses of this water body to the propagation of tides, tidal excursions and residual currents, the Cochin Estuary can be broadly classified into three zones:

- (i) A dynamic zone located between the Cochin inlet and Vaduthala (up to 22 km south), which represents the central estuary. The strong rectilinear currents are expected to maintain an effective flushing through the channel in this region.
- (ii) The region between Vaikom and Thanneermukkom (32 - 42 km) representing the south estuary, which represents a resonating water body. The south estuary experiences weak tidal currents due to the wide area south of Vaduthala. The region also show a tidal amplification when the hydraulic barrier at Thanneermukkom is closed.
- (iii) A zone located approximately 5-15 km north of the Cochin inlet, which oscillates differently to that in the south estuary. The tidal variations in this region are similar to that in the inlet. Consequently, the weak flow in the north estuary could be due to the synchronous tides entering through the two inlets which ultimately create a null zone (Ramamirtham and Muthusamy, 1986b).

The flow-restrictions are found to be primarily responsible for the sediment heavy metal contamination in the north estuary (Balachandran et al., 2005). Similarly, the drastic ecological changes observed in the south estuary, with disappearance of many economically important species, has been noted after the construction of hydraulic barrier at Thanneermukkom (Qasim, 2003). Recent investigations in the Cochin Estuary have collected a lot of environmental data, which on statistical analysis (PCA) has also shown the existence of three zones in the estuary (ICMAM, 2008). The present model confirms that these zones are topographic features of Cochin Estuary and could be responsible for its behavior as potential source of CO₂ into the atmosphere (Thottathil et al., 2008, Gupta et al., 2008). The zonal concept is a major finding suggesting that for the future development of the ecological model, integration of these zones is much needed.

6. Conclusions

The present study has achieved the objective of forming a basic 2D hydrodynamic model in predicting the propagation of tides for a complex estuarine system like the Cochin Estuary. The bathymetry applied in the model allows for simulations of tidal waves that are in good agreement with observations. According to model results, the Cochin Estuary can be classified into three distinctive zones with different tidal excursions. The model results would be useful in deciding locations for the disposal of industrial wastes to control pollution in the estuary. In conclusion, the zonal concept introduced is a significant contribution to the development of ecological model to Cochin Estuary.

Acknowledgments The authors thank Director, NIO, Goa, and Scientist-in-Charge, NIO, Cochin, for the encouragement and support. They are grateful to Director, ICMAM-PD, Ministry of Earth Sciences, Govt. of India, Chennai for the financial support given under the study “Ecosystem Modeling of Cochin backwaters”. The help received from the Marine Surveyor’s office, Cochin Port Trust, Cochin, State Irrigation Department, Thiruvananthapuram and Inland Waterway Authority of India, Cochin, for providing the sea level data are gratefully acknowledged. The critical suggestions by two anonymous reviewers and corrections made by Dr. Franciscus Colijn have substantially improved the clarity of the manuscript. This is NIO Contribution

References

- Joseph A, Balachandran KK, Mehra P, Prabhudesai RG, Dabolkar N, Vijaykumar, Revichandran C, Agarvadekar Y (2007a) Vulnerability of Cochin backwaters to meteorological disturbances with special reference to tidal propagation. *Emerging Trends in Meteorology and Oceanography METOC 2007*: 67-76.
- Joseph A, Mehra P, Sivadas TK, Prabhudesai RG, Srinivas K, Thottam TJ, Vijayan PR, Revichandran C, Balachandran KK (2007b) Identification of Msf tide amplification using a network of spatially distributed tide gauges. *Int. Symp. on Ocean Electronics SYMPOL-2007, Kochi*. 162-176.
- Babu MT, Vethamony P, Ehrlich Desa (2005) Modeling tide-driven currents and residual eddies in the Gulf of Kachchh and their seasonal variability: A marine environmental planning perspective. *Ecol Model* 184: 299-312.
- Babu MT, Kesvadas V, Vethamony P (2006) BOD-DO modeling and water quality analysis of a waste water outfall off Kochi, west coast of India. *Environ Internat* 32: 165-173.
- Balachandran KK, Laluraj CM, Nair M, Joseph T, Sheeba P, Venugopal P (2005) Heavy metal accumulation in a flow-restricted tropical estuary. *Estuar Coast Shelf Sci* 65: 361-370.
- Byun DS, Wang XH, Holloway PE (2004) Tidal characteristic adjustment due to dyke and seawall construction in the Mokpo Coastal Zone, Korea. *Estuar Coast Shelf Sci* 59: 185-196.
- Eldho TI, Naveen C (2004) Two dimensional hydrodynamic modeling of Cochin Estuary using finite element method. *INCHOE 2004, Nat. Inst. Oceanogr. Goa*.
- Emery WJ, Thompson RE (1997) *Data analysis methods in physical oceanography* (Pergamon Press, London).
- Gopalan UK, Doyil T Vengayil, Udaya Varma P, Krishnankutty M (1983) The shrinking backwaters of Kerala. *J Mar Biol Assn India* 25: 131-141.
- Gupta GVM, Thottathil SD, Balachandran KK, Robin RS, Madhu NV, Nair S (2008) Inorganic and organic carbon dynamics in a tropical eutrophic ecosystem (Cochin Estuary, India): Influence of plankton metabolism on CO₂ supersaturation. *Ecosystems* (under review).
- Kang JW, Jun KS (2003) Flood and ebb dominance in estuaries in Korea. *Estuar Coast Shelf Sci* 56: 187-196.
- Menon NN, Balchand AN, Menon NR (2000) Hydrobiology of the Cochin backwater system – a review. *Hydrobiol* 430: 149-183.

Integrated Coastal and Marine Area Management – Project Directorate (ICMAM-PD) - Ministry of Earth Sciences, Govt. of India (2008). Ecosystem Modeling of Cochin backwaters: Phase I Report.

Murray CB, Charitha B, Pattiaratchi, Gregory NI (2003) The tidal regime of Shark Bay, Western Australia. *Estuar Coast Shelf Sci* 57: 725 - 735.

Paul P, Cvetkovic V (2007) Modeling hydrodynamics of real world estuarine systems. Proc. COMSOL Conference 2007, Boston.

Priy CP, Narayana AC (2007) Particle size characterization and late Holocene depositional processes in Vembanad Lagoon, Kerala: Inferences from suit statistics. *J. Geol. Soc. India* 69, 311-318.

Pugh DT (1987) Tides, surges and mean sea level. John Wiley & Sons, Chichester.

Qasim SZ (2003) Cochin backwaters and Vembanad. In. S.Z.Qasim (eds) Indian estuaries, ISBN: 81-7764-369-X. Allied Publishers Pvt. Ltd., Mumbai, pp. 305-382.

Qingwen M, Ping Shi, Kedong Yin, Jianping Gan, Yiquan Qi (2004) Tides and tidal currents in the Pearl River Estuary. *Cont Shelf Res* 24: 1797-1808.

Ramaraju VS, Udayavarma P, Abraham Pylee (1979) Hydrographic characteristics and tidal prism at the Cochin harbour mouth. *Ind J Mar Sci* 8: 78-84.

Ramamirtham CP, Muthusamy S, Khambadkar LR (1986a) Estuarine oceanography of the Vembanad Lake. Part I: The region between Pallipuram (Vaikom) and Thevara (Cochin). *Ind J Fish* 33: 85-94.

Ramamirtham CP, Muthusamy S (1986b) Estuarine oceanography of the Vembanad Lake. Part II: The region between Cochin and Azhikode. *Ind J Fish* 33: 218-224.

Rasheed K (1997) Studies on dredging impact assessment at Cochin: A tropical estuarine harbour. Ph.D thesis, Cochin University of Science and Technology, India.

Reddy GS (1997) Aspects of a Computational Model for predicting the flow and pollutant transport in Rivers, Estuaries and Seas. *Computer Modeling of Seas and Coastal Regions*, Coast Engin. 97, La Coruna, Spain.

Shetye SR, Gouveia AD, Singbal SYS, Naik CG, Sundar D, Maichael GS, Nampoothiri G (1995) Propagation of tides in the Mandovi-Zuari estuarine network. *Proc Ind Acad Sci* 104: 667-682.

Soman K (1997) Geology of Kerala. Geological Society of India, Bangalore 1-278.

Srinivas K, Revichandran C, Maheswaran PA, Mohammed Ashraf TT, Nuncio M (2003a) Propagation of tides in the Cochin estuarine system, southwest coast of India. *Ind J Mar Sci* 32: 14-24.

Srinivas K, Revichandran C, Thottam TJ, Maheswaran PA, Mohammed Ashraf TT, Nuncio M (2003b) Currents in the Cochin estuarine system (southwest coast of India) during March 2000. *Ind J Mar Sci* 32: 123-132.

Strikwerda M (2004) Cochin Estuary morphological modeling and coastal zone management. Ph.D Thesis, University of Delft, Germany, pp.117.

Taguchi K, Nakata K (1998) Analysis of water quality in Lake Hamana using a coupled physical and biochemical model. *J Mar Sys* 16: 107-132.

Thompson JF, Thames FC, Martin CW (1977) TOMCAT- a code for numerical generation of body-fitted curvilinear coordinate system for filed containing any number of arbitrary two-dimensional bodies. *J Comp Phys* 15: 299-319.

Thottathil SD, Balachandran KK, Gupta GVM, Madhu NV, Nair S (2008). Influence of allochthonous input on autotrophic heterotrophic switch-over in shallow waters of a tropical estuary (Cochin Estuary), India. *Estuar. Coast. Shelf Sci.* (In Press).

Unnikrishnan AS, Shetye SR, Gouveia AD (1997) Tidal propagation in the Mandovi-Zuari estuarine network, west coast of India: Impact of Freshwater influx. *Estuar Coast Shelf Sci* 45: 737-744.

Varma PU, Pylee A, Ramaraju VS (1981) Tidal influence on the seasonal variation in current and salinity around Willingdon Island. *Mahasagar – Bull Nat Inst Oceanogr* 14: 225-237.

Varma KK, Cherian CJ, Mrithunjayan PS, Raman NN, Prabha J (2002) Characteristics of temperature and salinity fluctuations in a South Indian Estuary (A study of Vembanal Lake, a monsoon-influenced estuary). *Earth Sys Mon* 12: 9-14.

Vethamony P, Reddy GS, Babu MT, Desa E, Sudheesh K (2005) Tidal eddies in a semi-enclosed basin: a model study. *Mar Env Res* 59: 519-532.

Wyatt T, Qasim SZ (1973) Application of a model to an estuarine ecosystem. *Lim Oceanogr* 18: 301-306.

Ye Longfei, John AJ (1994) Models of Kelvin tidal waves in the Lingdingyang Region, Pearl River Estuary, South China. *Estuar Coast Shelf Sci* 38: 291-299.

Table.1. Statistics of observed versus predicted water level at various stations

Month	Locations	r^2	SD (m)	n	RMS Error (m)	Observed maximum range (m)	Predicted maximum range (m)
Mar-04	CPT	-	-	-	-	1.01	-
	Thevara	0.68	0.11	325	0.13	0.69	0.59
	Vaduthala	0.88	0.05	325	0.07	0.63	0.52
	M.Kadavu	0.86	0.06	325	0.06	0.53	0.53
	Vaikom	0.80	0.07	325	0.09	0.72	0.53
	TVPuram	0.79	0.07	325	0.09	0.70	0.54
	Thanneer- mukkom	0.65	0.09	325	0.10	0.62	0.54
Oct-03	CPT	-	-	-	-	1.15	-
	Thevara	0.51	0.08	373	0.11	0.57	0.5
	Vaduthala	0.68	0.05	373	0.06	0.46	0.33
	M.Kadavu	0.63	0.05	373	0.06	0.30	0.32
	Vaikom	0.59	0.06	373	0.07	0.36	0.34
	TVPuram	0.73	0.05	373	0.05	0.42	0.35
	Thanneer- mukkom	0.53	0.06	373	0.07	0.42	0.35

n – number of observations, r – correlation coefficient;
RMS – root mean square error

Legends to figures

Fig. 1. Topography of Cochin Estuary showing tidal stations and interpolated bathymetry depths (m). The dotted lines indicate the model domain

Fig.2. Computational BFC grid of a sub region in the domain

Fig.3. (a) Observed tides at Cochin Port Trust (b) Comparison of observed vs. predicted tides and (c) Comparison of observed vs. predicted along-shore currents at Bolghatty during March 2004

Fig.4. Comparison of computed and observed tidal elevations (m) at various locations in the Cochin Estuary during March 2004.

Fig.5. Comparison of computed and observed tidal elevations (m) at various locations in the Cochin Estuary during October 2003.

Fig.6. Computed tidal levels and current vectors in Cochin Estuary during an ebb tide of October 2003 (dynamic zone marked by “ \longleftrightarrow ”).

Fig.7. Computed tidal levels and current vectors in Cochin Estuary during an ebb tide of March 2004 (dynamic zone marked by “ \longleftrightarrow ”).

Fig.8. Residual currents of 14.5-day period during October 2003 (dynamic zone marked by “ \longleftrightarrow ”).

Fig.9. Tidal excursion visualized by the Lagrangean particle movement. The trajectories of particles released at 10 locations in the estuary after 14.5 days of simulations in (a) October 2003 and (b) March 2004.

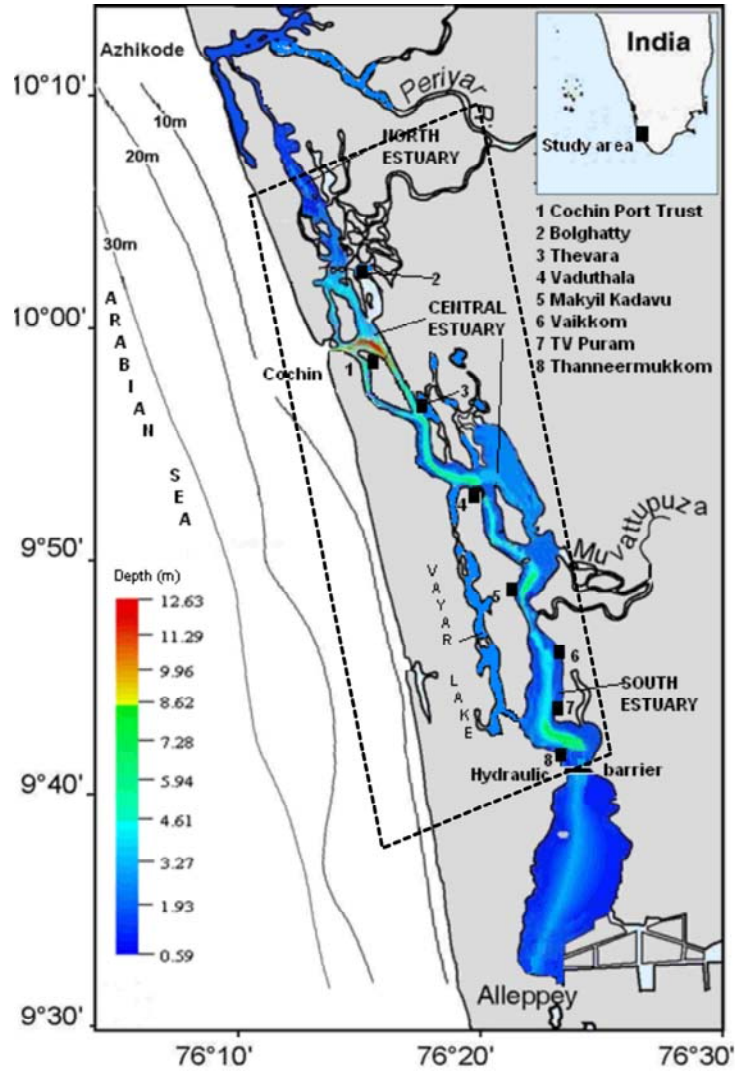


Fig. 1. Topography of Cochin Estuary showing tidal stations and interpolated bathymetry depths (m). The dotted lines indicate the model domain.

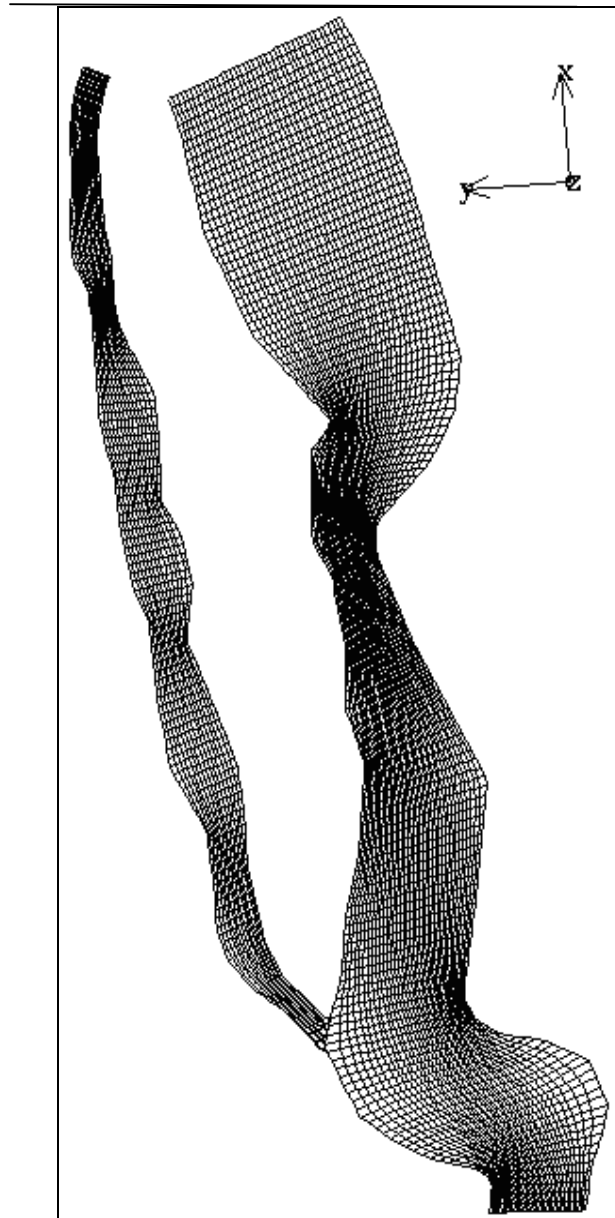


Fig.2. Computational BFC grid of a sub region in the domain

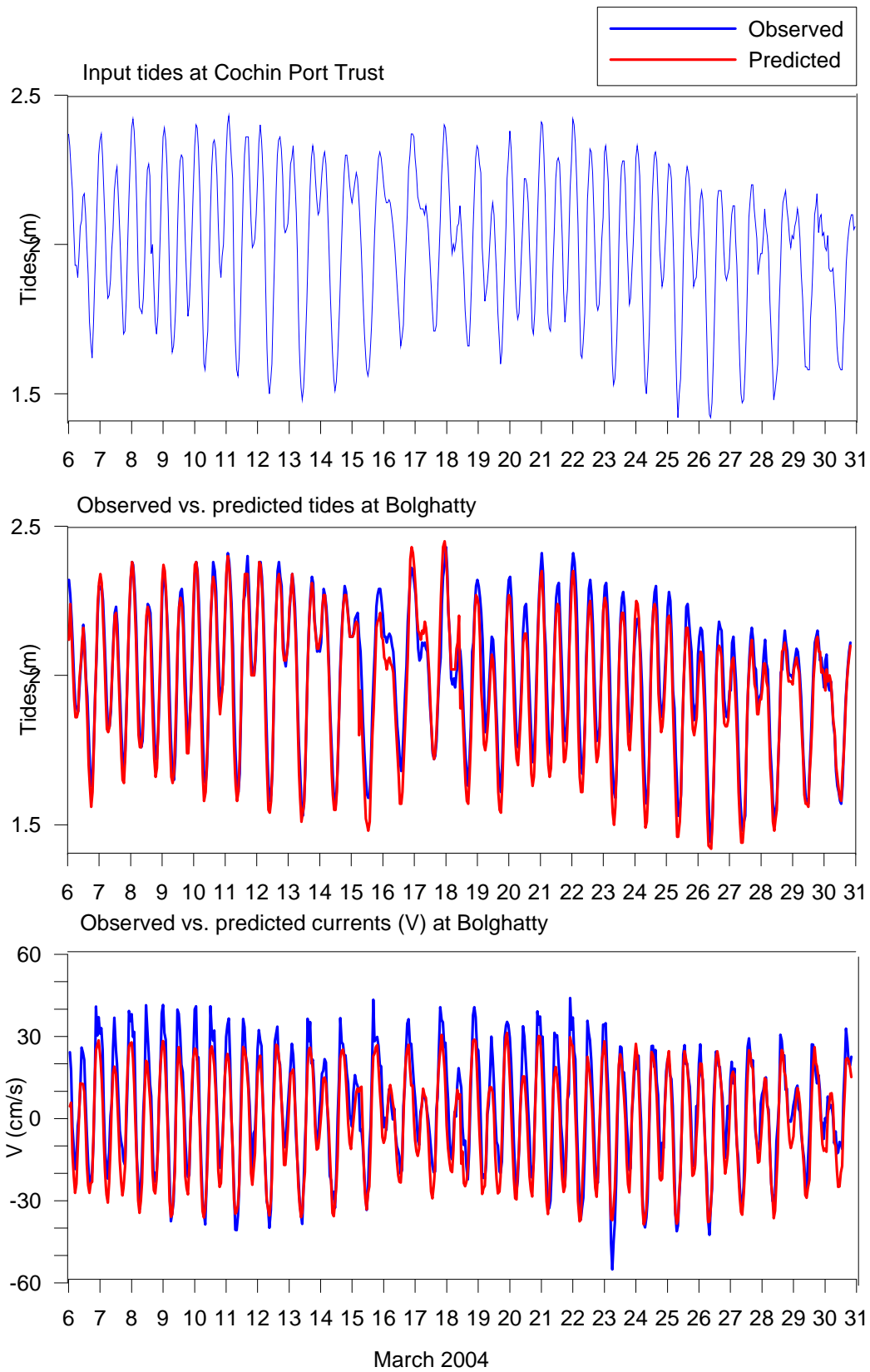


Fig. 3 (a) Observed tides at CPT (b) Comparison of observed vs. predicted tide at Bolghatty and (c) Observed vs. predicted along shore currents at Bolghatty during March 2004

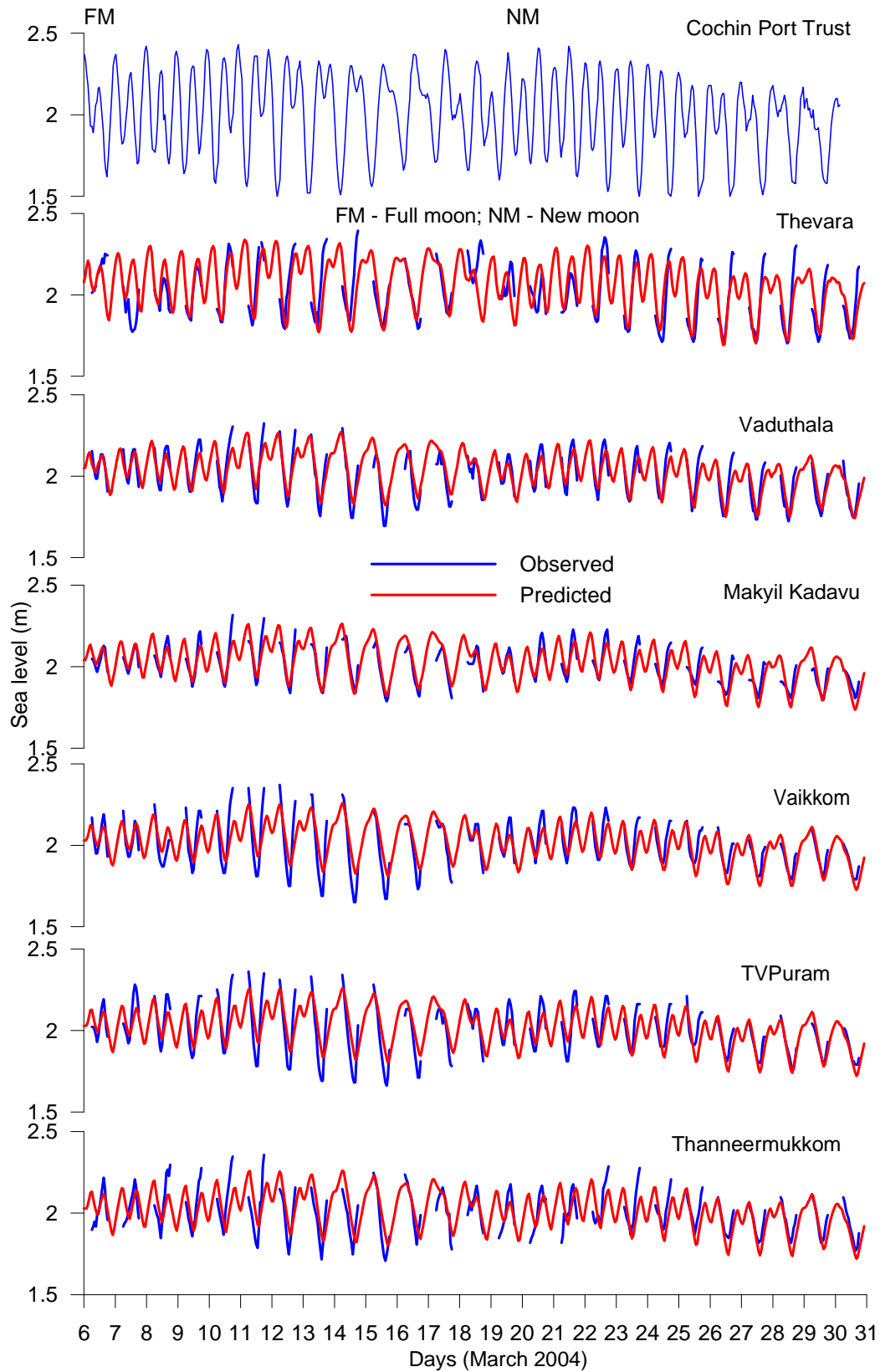


Fig.4. Comparison of computed and observed tidal elevations at various locations in the Cochin Estuary during March 2004.

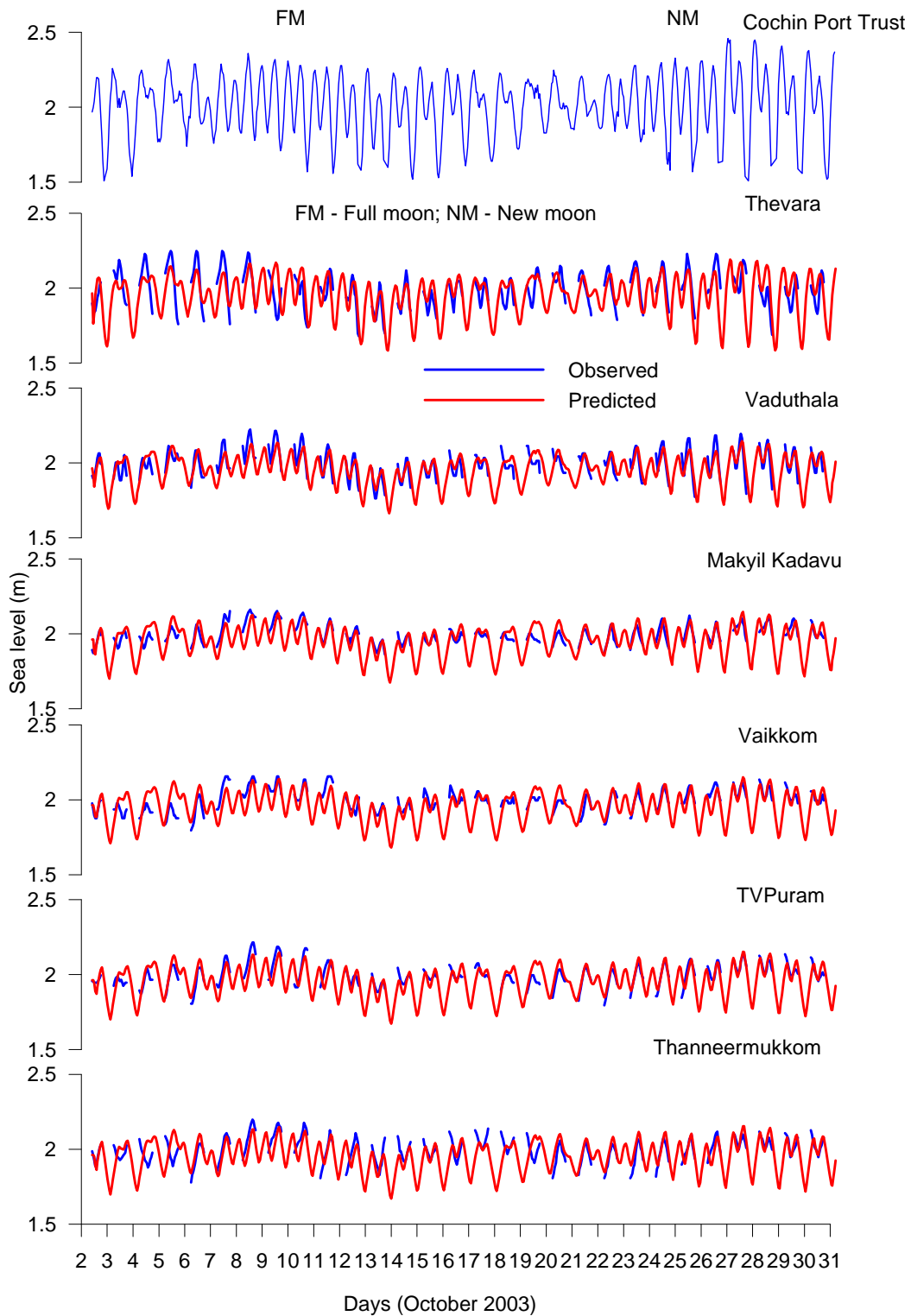


Fig.5. Comparison of computed and observed tidal elevations at various locations in the Cochin Estuary during October 2003.

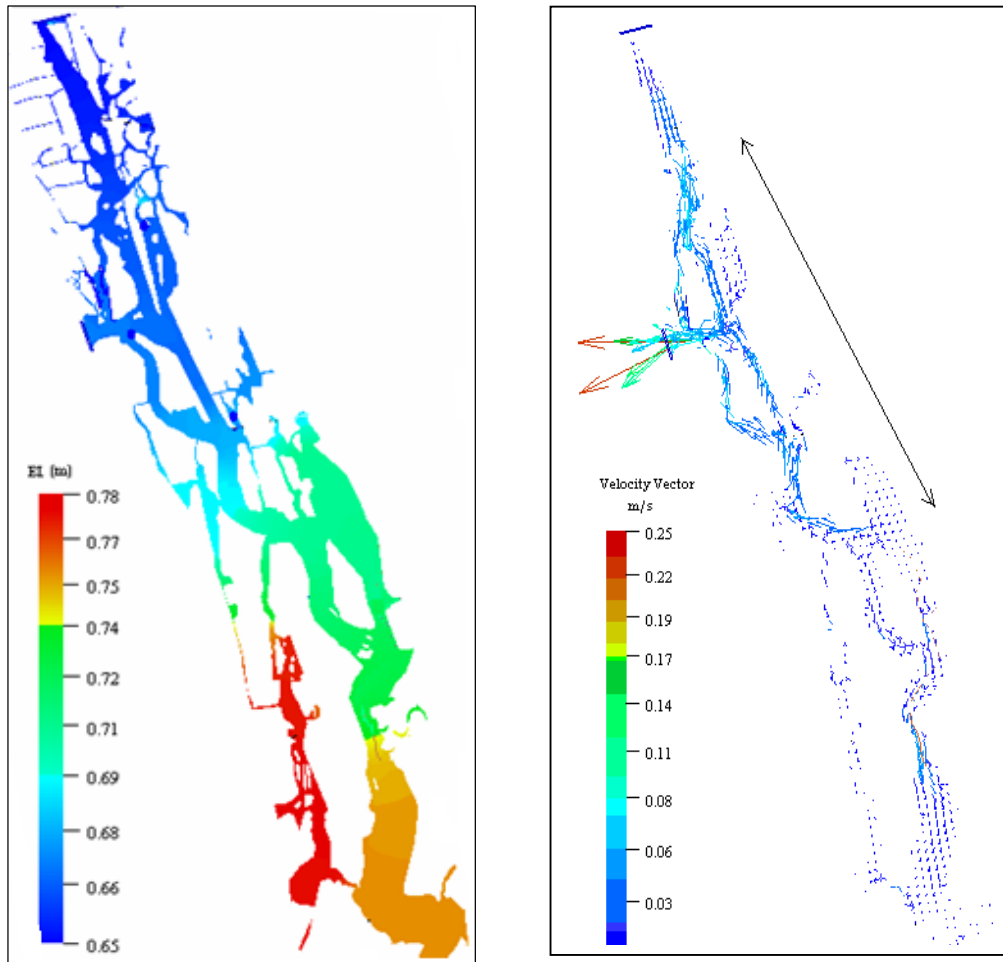


Fig.6. Computed tidal levels and current vectors in Cochin Estuary during an ebb tide of October 2003 (dynamic zone marked by “ \longleftrightarrow ”)

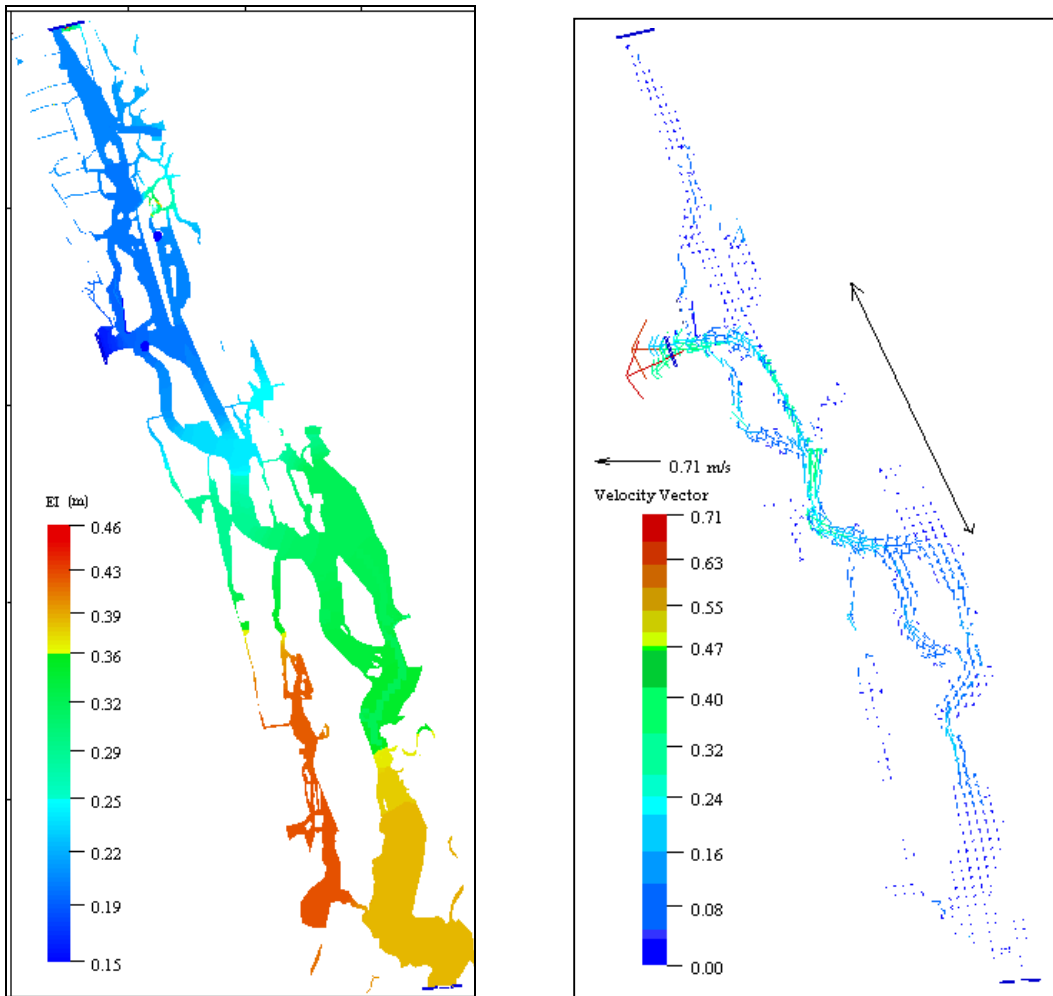


Fig.7. Computed tidal levels and current vectors in Cochin Estuary during an ebb tide of March 2004 (dynamic zone marked by “ \leftrightarrow ”)

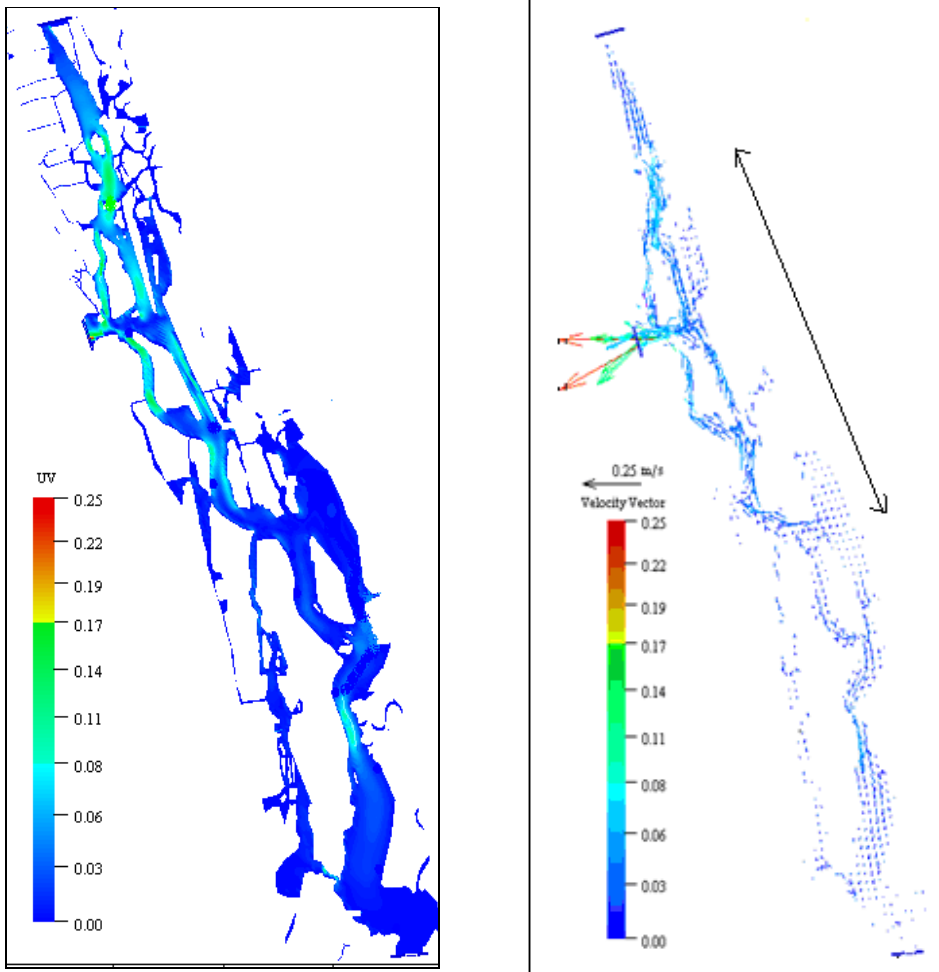


Fig.8. Residual currents of 14.5-day period during October 2003
(dynamic zone marked by “ \longleftrightarrow ”)

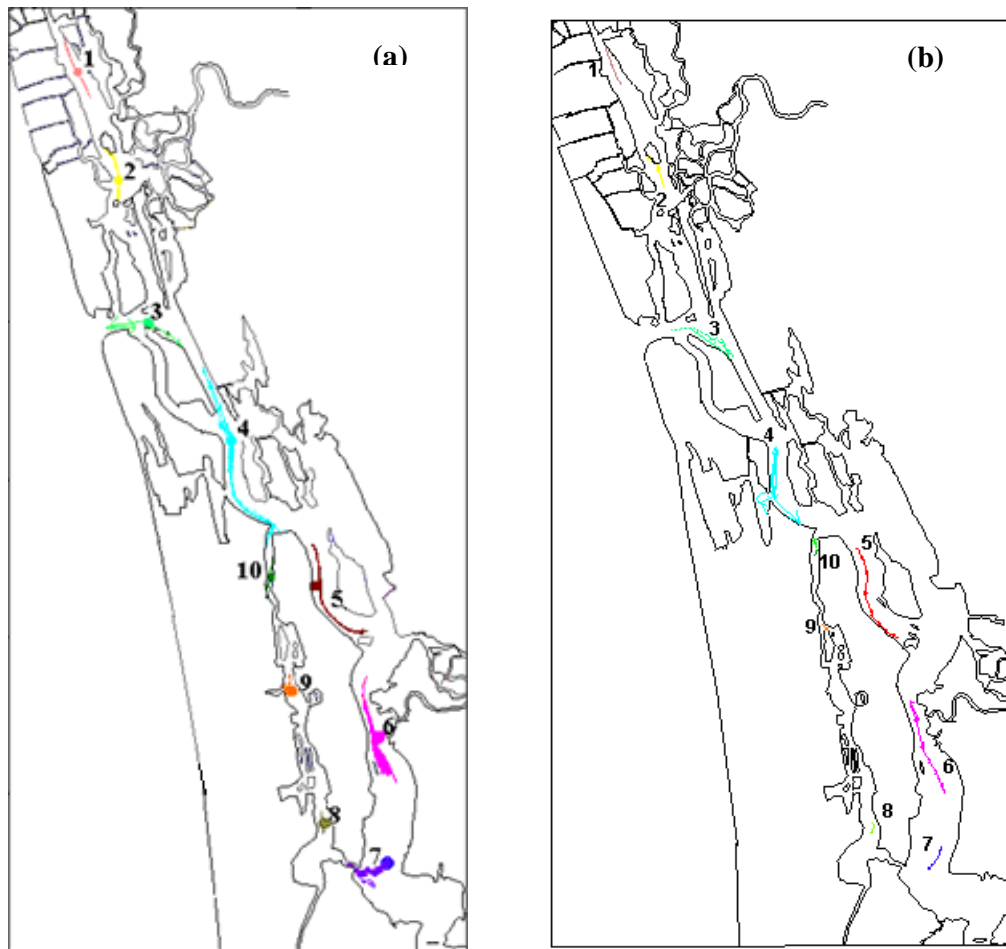


Fig.9. Tidal excursion visualized by the Lagrangean particle movement. The trajectories of particles released at 10 locations in the estuary after 14.5 days of simulations in (a) October 2003 and (b) March 2004.